

# Improving the adaptability of an active power filter using linearization feedback input-output sliding mode

Leminh Thien Huynh<sup>1</sup>, Van-Cuu Ho<sup>1</sup>, Thanh-Vu Tran<sup>2</sup>

<sup>1</sup>Faculty of Engineering and Technology, Saigon University, Ho Chi Minh City, Vietnam

<sup>2</sup>Institute of Information Technology and Electrical-Electronics, University of Transport, Ho Chi Minh City, Vietnam

## Article Info

### Article history:

Received Oct 16, 2023

Revised Aug 7, 2025

Accepted Oct 16, 2025

### Keywords:

Active power filter

Adaptive control

Power quality

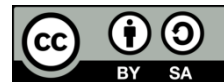
Sliding mode

Slip control

## ABSTRACT

As more and more non-linear loads are used in industrial applications, power quality problems become more serious. To address this challenge, a robust nonlinear control strategy is introduced using an active power filter (APF) to enhance the power quality of the three-phase neutral voltage. The system employs a control algorithm tailored for a three-phase split-capacitor inverter, which eliminates high-order harmonics through a voltage source inverter (VSI) equipped with an LCL filter. The grid-side components of the LCL filter are incorporated into a sliding mode control framework to minimize oscillations while maintaining performance. Additionally, the d-q-0 transformation within the synchronous reference frame is applied to effectively manage the second harmonic component. In addition, the linear feedback input-output sliding mode facilitates the control system. This system can help decrease total harmonic distortion (THD) to meet IEEE-519 standards. This method demonstrates its effectiveness through simulation results, reducing THD to less than 5% and defeating previous methods despite still using simple algorithms.

*This is an open access article under the [CC BY-SA](https://creativecommons.org/licenses/by-sa/4.0/) license.*



## Corresponding Author:

Leminh Thien Huynh

Faculty of Engineering and Technology, Saigon University

273 An Duong Vuong Street, Ward Cho Quan, Ho Chi Minh City, Vietnam

Email: leminhthien.huynh@sgu.edu.vn

## 1. INTRODUCTION

In today's industrial landscape, the increasing use of nonlinear loads has a significant impact on power quality. These systems are required to comply with standards such as IEEE 519-2014, IEC 61000-3-2, and IEC 61000-3-4 [1]. With advancements in microelectronic technology, such loads produce non-sinusoidal currents that introduce harmonics into the power system, making high-quality power supplies essential.

Active power filters (APFs) not only improve power quality but also serve as an effective solution for mitigating harmonics and other disturbances. As a result, APF controllers have rapidly become a widely adopted tool for optimizing power quality. For instance, a dedicated three-phase inverter with a current controller has been developed to enhance power quality for unbalanced nonlinear loads, eliminating the need for an additional switching branch to regulate neutral current [2].

Leveraging voltage source inverters (VSIs), APFs enhance power quality by reshaping input harmonic reference signals [3], [4]. Complex nonlinear load applications—such as electric transportation systems and solar power installations—often demand highly stable and clean power supplies [5]-[9]. These loads may result in either balanced or unbalanced three-phase conditions that fail to meet standard requirements, leading to the emergence of zero-sequence and reverse-sequence currents. These negative-sequence components can cause motor overheating, transformer saturation, power outages, and compromise

the safety of neutral lines. To address these challenges, a decoupling-capacitor-neutral-point VSI configuration suitable for APF integration is employed, offering a reliable approach to maintaining system stability and power quality.

The flexibility and performance of conventional APF control methods often suffer from problems under different load conditions. To deal with this problem, an advanced APF control method using linearization feedback input-output sliding mode (LF-IOSM) is proposed. This system improves the flexibility and efficiency of APF, efficiently decreases total harmonic distortion (THD), and complies with power quality standards.

Voltage source inverters (VSIs) are commonly employed in three-phase grid systems integrated with active power filters (APFs). These systems can be connected to loads using a four-wire VSI configuration with neutral grounding. One method for establishing a neutral point involves using a  $\Delta/Y$  transformer, where the  $\Delta$  side connects to the VSI and the  $Y$  side to the load [8]-[11]. However, this approach requires a bulky, heavy, and costly transformer.

An alternative technique utilizes three-phase split-capacitor VSIs and four-pin VSIs, comprising a total of 16 switches. In [12], [13], the four-pin inverter design includes two additional switches, which are essential for implementing complex 3D space vector modulation. A three-phase, four-wire system can also be derived from a conventional three-phase, three-wire VSI by incorporating a DC voltage divider. In this configuration, the neutral point serves as the fourth wire, enabling space vector modulation. This setup allows for output voltage regulation and facilitates the flow of zero-sequence current through the neutral conductor.

Recent research has focused on maintaining stable output from three-phase inverters under unbalanced load conditions. For example, Chen *et al.* [14] employed deadbeat control with current and voltage feedback to compensate for coil losses, though this method does not address harmonic distortion. Geng *et al.* [15] introduced repetitive control to suppress periodic disturbances in nonlinear systems, but its slow response and limited applicability pose challenges.

Other control strategies, such as sliding mode control, have demonstrated improved APF performance under uncertain grid conditions [3], [11], [16]-[20]. Discrete sliding mode control offers excellent dynamic response, reduced sensitivity to load variations, and robust stability. To manage asymmetric three-phase signals, the symmetric constant-distribution method is used in conjunction with a proportional-integral (PI) controller to balance inverter output voltage [21]. However, PI controllers increase computational complexity, making them more suitable for nonlinear and unbalanced load scenarios [22].

This paper presents a detailed investigation into the development and implementation of the linearization feedback input-output sliding mode (LF-IOSM) control method for APFs. Extensive simulation results validate the effectiveness of the proposed approach across diverse operating conditions. Recent studies [3]-[7] provide a solid foundation for this work. Figure 1 illustrates the schematic of the active power filter system.

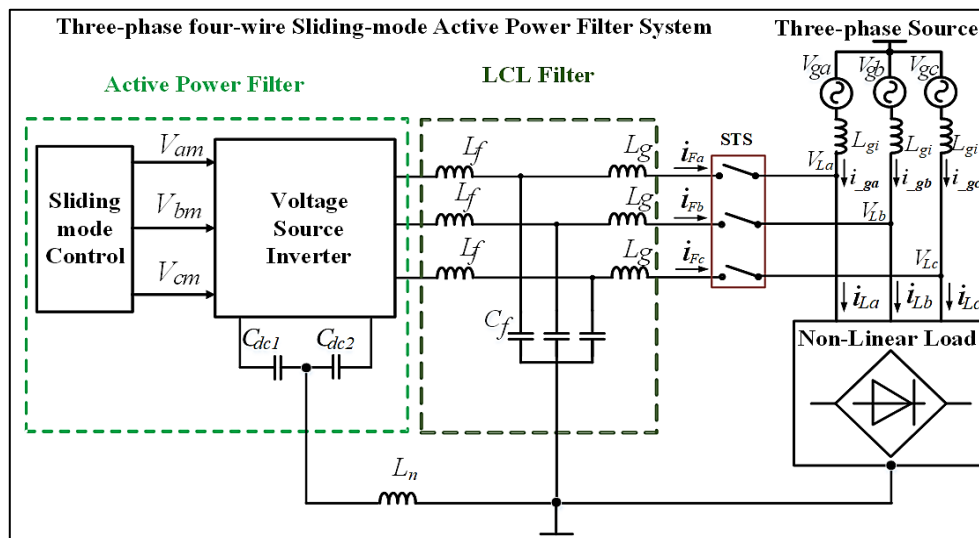


Figure 1. Sliding mode control for three-phase active power filter systems

Assuming the three-phase generator is unbalanced, Kirchhoff's first law can be applied to the system. Using this law, the single-phase current can be calculated as shown in (1).

$$i_{ga} = i_{La} - i_{Fa} \quad (1)$$

Let  $i_{ga}$  represent the current in phase  $a$ ,  $i_{La}$  the load current in phase  $a$ , and  $i_{Fa}$  the current injected by the active power filter (APF) into the grid in phase  $a$ . The APF generates currents  $i_{Fa}$ ,  $i_{Fb}$ , and  $i_{Fc}$  that satisfy Kirchhoff's first law, as described in (1)-(3). These APF-generated currents effectively eliminate most of the high-order harmonics produced by nonlinear loads. Applying the same principle to phases  $b$  and  $c$ , the corresponding currents for these phases are also determined using (2) and (3).

$$i_{gb} = i_{Lb} - i_{Fb} \quad (2)$$

$$i_{gc} = i_{Lc} - i_{Fc} \quad (3)$$

In a four-wire system with unbalanced loads, the three-phase power source becomes distorted by harmonics, leading to reduced power quality and potential damage to electrical and electronic devices. These harmonics can be represented by (4), where  $n$  denotes the harmonic order [23].

$$\begin{aligned} i_{gan}(t) &= \sqrt{2}I_{0n} \sin(\omega_n t + \psi_{0n}) + \sqrt{2}I_{+n} \sin(\omega_n t + \psi_{+n}) + \sqrt{2}I_{-n} \sin(\omega_n t + \psi_{-n}) \\ i_{gbn}(t) &= \sqrt{2}I_{0n} \sin(\omega_n t + \psi_{0n}) + \sqrt{2}I_{+n} \sin(\omega_n t + \psi_{+n} - \frac{2\pi}{3}) + \sqrt{2}I_{-n} \sin(\omega_n t + \psi_{-n} + \frac{2\pi}{3}) \\ i_{gcn}(t) &= \sqrt{2}I_{0n} \sin(\omega_n t + \psi_{0n}) + \sqrt{2}I_{+n} \sin(\omega_n t + \psi_{+n} + \frac{2\pi}{3}) + \\ &\quad \sqrt{2}I_{-n} \sin(\omega_n t + \psi_{-n} - \frac{2\pi}{3}) \end{aligned} \quad (4)$$

The primary objective of the active power filter (APF) system is to reduce total harmonic distortion (THD). Non-linear loads generate high-frequency components that contribute to THD, which is called  $THD_{sm}$ . According to IEEE Std. 519, the  $THD_{sm}$  of the source current should be kept below 5%.  $THD_{sm}$  quantifies the harmonic distortion by calculating the ratio of the sum of all harmonic currents ( $I_2, I_3, I_4, \dots, I_n$ ) to the fundamental current ( $I_1$ ), expressed as a percentage, as illustrated in (4).

$$THD_{sm} = \sqrt{\frac{I_2^2 + I_3^2 + I_4^2 + \dots + I_n^2}{I_1^2}} \cdot 100\% \quad (5)$$

This paper introduces an advanced nonlinear control strategy for a three-phase voltage source inverter (VSI), utilizing input-slip feedback to achieve output linearization under both balanced and unbalanced nonlinear load conditions. To streamline computation and reduce hardware complexity, sliding mode control theory is employed. The proposed method effectively suppresses high-order harmonics and lowers total harmonic distortion (THD) in nonlinear loads, as validated by simulation results. The structure of the paper is as follows: section 2 presents the mathematical modeling, section 3 details the input-output linearization feedback system model, section 4 showcases the simulation outcomes, and section 5 provides discussion and conclusions.

## 2. MODEL-BASED SYSTEM ANALYSIS

Figure 2 illustrates the three-phase active power filter (APF) configured with a split-capacitor neutral point voltage source inverter (VSI) topology. In the  $d-q-0$  coordinate system [24], [25], according to the unbalanced loads, the zero-sequence components are given by (6) and (7).

$$i_{dq} = \frac{v_{dq}}{L_g} - \frac{v_{ldq}}{L_g} - j\omega i_{dq}, i_0 = \frac{(v_0 - v_{l0})}{(L_g + 3L_n)} \quad (6)$$

$$\dot{v}_{ldq} = \frac{(i_{dq} - i_{ldq})}{C_f} - j\omega v_{ldq}, \dot{v}_{l0} = \frac{(i_0 - i_{l0})}{C_f} \quad (7)$$

Here,  $L_g$  denotes the grid-side inductor in inductor-capacitor-inductor (L-C-L) filter configuration;  $L_n$  represents the neutral wire filter;  $C_f$  is the filter capacitor;  $v_{dq}$  and  $v_0$  are the output voltage components of the VSI in the  $d-q-0$  reference frame;  $i_d$ ,  $i_q$ , and  $i_0$  are the transformed switching current components derived from  $i_{Fj}$  (where  $j=a,b,c$ ) into the  $d-q-0$  coordinate system;  $i_{ld}$ ,  $i_{lq}$ , and  $i_{l0}$  are the load current components; and  $\omega$  is the angular frequency of the power source. Based on (6) and (7), the system's state-space model can be formulated as (8).

$$\dot{x} = Ax + Bv - \frac{i_l}{C_f} \tag{8}$$

In which:  $x = [i_d, i_q, i_o, i_{ld}, i_{lq}, i_{ln}]^T$  is the state vector,  $v = [v_d, v_q, v_n]^T$  is the input from the source, and  $i_l = [0, 0, 0, i_{ld}, i_{lq}, i_{ln}]^T$  is the load current.  $A$  and  $B$  are the coefficient matrices extracted from the original expression:  $A = \omega A_\omega + L_g^{-1} A_L + (L_g + 3L_n)^{-1} A_n + C_f^{-1} A_C$  and  $B = \text{diag}(L_g^{-1}, L_g^{-1}, (L_g + 3L_n)^{-1}, 0, 0)$ , where  $A_\omega$  contains elements related to  $\omega$ ,  $A_L$  contains elements related to  $L_g^{-1}$ ,  $A_n$  element contains a single element related to  $(L_g + 3L_n)^{-1}$ , and  $A_C$  contains elements related to  $C_f^{-1}$ .

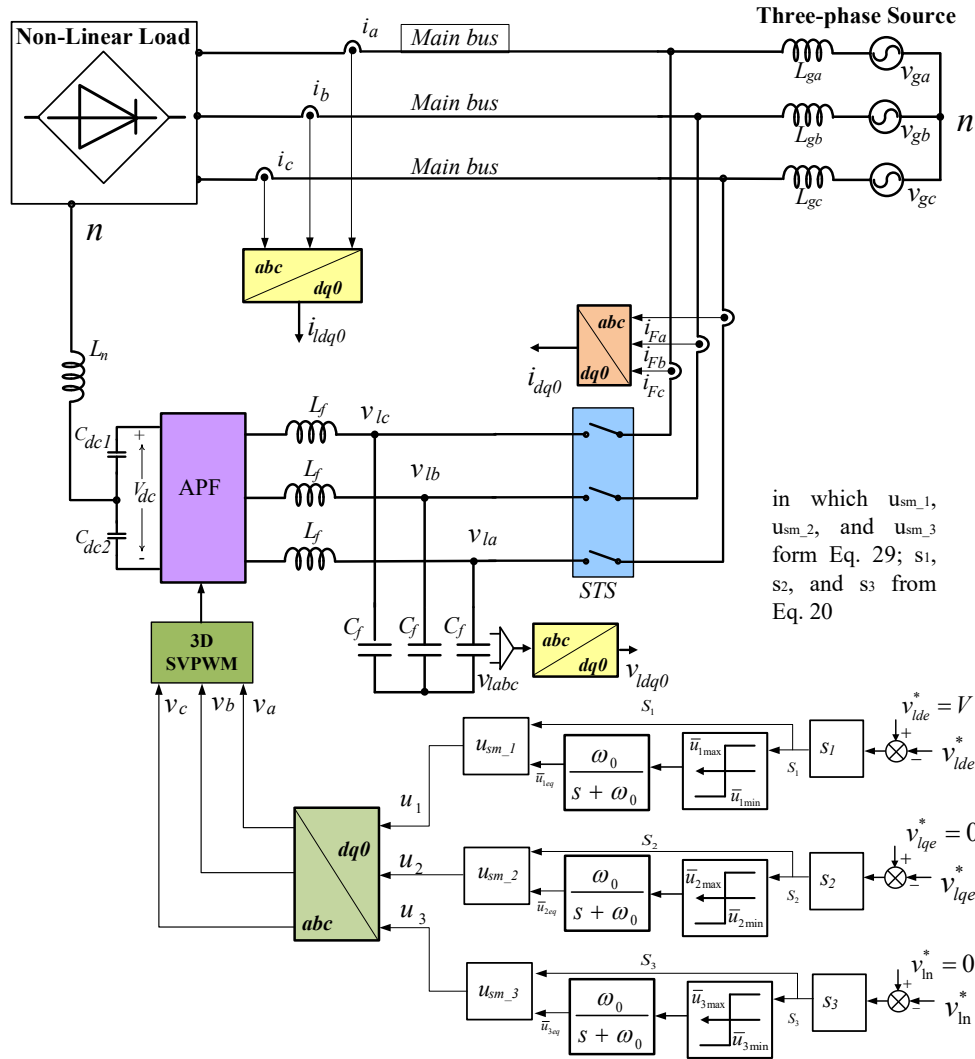


Figure 2. Layout of three-phase APF using sliding mode

### 3. FEEDBACK REGULATION WITHIN THE SLIDING MODE FRAMEWORK

#### 3.1. Control of input and output using feedback linearization

The linear multi-input multi-output (MIMO) access controller was proposed to eliminate nonlinear behavior in the simulation model [26], [27]. The following equations represent the corresponding MIMO control framework:

$$\dot{x}_{sm} = f(x_{sm}) + g_{sm} \cdot u_{sm} \tag{9}$$

$$y_{sm} = h(x_{sm}) \tag{10}$$

where  $x_{sm}$  denotes the state vector,  $u_{sm}$  represents the control input,  $y_{sm}$  is the system output,  $f$  and  $g$  are smooth matrix functions, and  $h$  is a smooth scalar function. The dynamic behavior of the VSI, as defined in (10), is formulated through (9) to (12) [27].

$$x_{sm} = [i_d i_q i_0 v_{ld} v_{lq} v_{ln}]^T; u_{sm} = [v_d v_q v_n]^T; y_{sm} = [v_{ld} v_{lq} v_{ln}]^T$$

$$g_{sm} = \frac{1}{L_g C_f} \cdot \text{diag} \left( 1, 1, \frac{L_g}{L_g + 3L_n} \right) \tag{11}$$

$$f(x_{sm}) = [\prod_{k=1,6} f_k(x_{sm})]^T, \text{ in which:}$$

$$f_1(x_{sm}) = \omega i_q - \frac{v_{ld}}{L_g}, f_2(x_{sm}) = -\omega i_q - \frac{v_{ld}}{L_g}, f_3(x_{sm}) = \frac{v_{ln}}{(L_g + 3L_n)}$$

$$f_4(x_{sm}) = \frac{i_d}{C_f} - i_{ld} + \omega v_{lq}, f_5(x_{sm}) = \frac{i_q - i_{lq}}{C_f} - \omega v_{ld}, f_6(x_{sm}) = \frac{i_n - i_{ln}}{C_f} \tag{12}$$

To create a direct mapping between the outputs  $y_{sm_i}$  for  $i=1, 2, 3$  and the inputs  $u_{sm_i}$  for  $i=1, 2, 3$ , each output is systematically varied until a corresponding control input is triggered.

$$\begin{bmatrix} \ddot{y}_{sm_1} \\ \ddot{y}_{sm_2} \\ \ddot{y}_{sm_3} \end{bmatrix} = A(x_{sm}) + E(x_{sm}) \begin{bmatrix} u_{sm_1} \\ u_{sm_2} \\ u_{sm_3} \end{bmatrix} \tag{13}$$

The control strategy is defined as:

$$A(x_{sm}) = \frac{1}{C_f} \cdot \begin{bmatrix} 2\omega i_d - \gamma_d \\ -2\omega i_d - \gamma_q \\ \chi v_{ln} - \dot{i}_{ln} \end{bmatrix} \left| \begin{array}{l} \gamma_d = (L_g^{-1} + \omega^2 C_f) v_{ld} - \dot{i}_{ld} - \omega i_{lq} \\ \gamma_q = (L_g^{-1} + \omega^2 C_f) v_{lq} - \dot{i}_{ld} + \omega i_{ld} \\ \chi = -(L_g + 3L_n)^{-1} \end{array} \right. \tag{14}$$

$$E^{-1}(x_{sm}) = L_g C_f \cdot \text{diag} \left( 1, 1, (1 + 3L_n \cdot L_g^{-1}) \right) \tag{15}$$

where:

$$\det[E(x_{sm})] = \frac{1}{(L_g + 3L_n) L_g^2 C_f^3} \neq 0 \tag{16}$$

To satisfy the requirements of dynamic systems, the expected values of dynamic responses are required. These values can be determined using (17).

$$\begin{bmatrix} v_1 \\ v_2 \\ v_3 \end{bmatrix} = \begin{bmatrix} \ddot{y}_{sm_1ref} - \eta_{11} \dot{e}_1 - \eta_{12} e_1 \\ \ddot{y}_{sm_2ref} - \eta_{21} \dot{e}_1 - \eta_{22} e_1 \\ \ddot{y}_{sm_3ref} - \eta_{31} \dot{e}_1 - \eta_{32} e_1 \end{bmatrix} \tag{17}$$

In this context,  $e_1 = y_{sm1}^* - y_{sm1}$ ,  $e_2 = y_{sm2}^* - y_{sm2}$ , and  $e_3 = y_{sm3}^* - y_{sm3}$ , where  $y_{sm1}^*$ ,  $y_{sm2}^*$ , and  $y_{sm3}^*$  represent the reference values corresponding to  $y_{sm1}$ ,  $y_{sm2}$ , and  $y_{sm3}$ , respectively. The error dynamics are described in (13) through (19).

$$\begin{aligned} \ddot{e}_{1ref} + \eta_{11} \dot{e}_1 + \eta_{12} e_1 &= 0 \\ \ddot{e}_{2ref} + \eta_{21} \dot{e}_1 + \eta_{22} e_1 &= 0 \\ \ddot{e}_{3ref} + \eta_{31} \dot{e}_1 + \eta_{32} e_1 &= 0 \end{aligned} \tag{18}$$

The error dynamics are ensured when the gain coefficients  $\eta_{11}$ ,  $\eta_{12}$ ,  $\eta_{21}$ ,  $\eta_{22}$ ,  $\eta_{31}$ , and  $\eta_{32}$  are all positive. The controller input in (13) reflects the concept of integrated control as (19).

$$[u_{sm_i}] = L_g C_f \cdot [\mu_i] \left| [u_{sm_i}] = \begin{bmatrix} u_{sm_1} \\ u_{sm_2} \\ u_{sm_3} \end{bmatrix}, \text{ and } [\mu_i] = \begin{bmatrix} \mu_1 \\ \mu_2 \\ \mu_3 \end{bmatrix} \right. \tag{19}$$

In which:

$$\begin{aligned}\mu_1 &= v_1 - 2\omega i_q \cdot C_f^{-1} + \left( (L_g C_f)^{-1} + \omega^2 \right) v_{ld} + \dot{i}_{ld} \cdot C_f^{-1} + i_{lq} \omega \cdot C_f^{-1} \\ \mu_2 &= v_2 + 2i_d \omega \cdot C_f^{-1} + \left( (L_g C_f)^{-1} + \omega^2 \right) v_{lq} + \dot{i}_{lq} \cdot C_f^{-1} - i_{ld} \omega \cdot C_f^{-1} \\ \mu_3 &= \left( 1 + 3L_n L_g^{-1} \right) \left( v_3 + \left[ (L_g + 3L_n) C_f \right]^{-1} v_{ln} + \dot{i}_{ln} \cdot C_f^{-1} \right)\end{aligned}$$

Although the voltages  $v_{ld}$ ,  $v_{lq}$ , and  $v_{ln}$  are linearized, implementing a digital processor capable of handling complex operations like derivatives and differentials remains challenging. As a result, the derivatives of the electrical currents  $i_{ld}$ ,  $i_{lq}$ , and  $i_{ln}$  continue to emerge within the circuit. To address this issue, a controller based on sliding mode theory is proposed. This approach enables the design of a linearized feedback input-output control system using consistent communication and weighting parameters, simplifying implementation [13], [28], [29].

### 3.2. Sliding mode controller based on linearized input-output feedback

As a result of faults in the indirect voltage device, the sliding mode controller surfaces are affected. These surfaces are determined using (20).

$$\begin{aligned}s_1 &= \dot{e}_1 + \eta_{11} e_1 + \eta_{12} \int e_1 dt \\ s_2 &= \dot{e}_2 + \eta_{21} e_2 + \eta_{22} \int e_2 dt \\ s_3 &= \dot{e}_3 + \eta_{31} e_3 + \eta_{32} \int e_3 dt\end{aligned}\quad (20)$$

If the system states operate along a specific surface, then  $s_1 = s_2 = s_3 = 0$  and (20) can be reformulated in the following matrix form:  $\dot{s}_1 = \dot{s}_2 = \dot{s}_3 = 0$ .

$$\begin{aligned}\ddot{e}_1 &= -\eta_{11} \dot{e}_1 - \eta_{12} e_1 \\ \ddot{e}_2 &= -\eta_{21} \dot{e}_2 - \eta_{22} e_2 \\ \ddot{e}_3 &= -\eta_{31} \dot{e}_3 - \eta_{32} e_3\end{aligned}\quad (21)$$

The (21) ensures that the system states  $v_{ld}$ ,  $v_{lq}$ , and  $v_{ln}$  will converge to their reference power values when constrained to the zero sliding surface [30]. On this surface, where  $s = \dot{s} = 0$ , the equivalent control acts as a conventional controller that facilitates trajectory tracking. The equivalent control law is defined as (22).

$$\begin{aligned}\dot{s}_1 &= \ddot{e}_1 + \eta_{11} \dot{e}_1 + \eta_{12} e_1 \\ \dot{s}_2 &= \ddot{e}_2 + \eta_{21} \dot{e}_2 + \eta_{22} e_2 \\ \dot{s}_3 &= \ddot{e}_3 + \eta_{31} \dot{e}_3 + \eta_{32} e_3\end{aligned}\quad (22)$$

Where  $v_1$ ,  $v_2$ , and  $v_3$  correspond to the newly defined inputs of the system, as illustrated in (23).

$$\begin{aligned}v_1 &= \ddot{v}_{cdref}^* + \eta_{11} \dot{e}_1 + \eta_{12} e_1 \\ v_2 &= \ddot{v}_{cqref}^* + \eta_{21} \dot{e}_2 + \eta_{22} e_2 \\ v_3 &= \ddot{v}_{c0ref}^* + \eta_{31} \dot{e}_3 + \eta_{32} e_3\end{aligned}\quad (23)$$

Ultimately, the equivalent control phase is realized by enforcing the condition  $\dot{s}_1 = \dot{s}_2 = \dot{s}_3 = 0$ . The corresponding control expression is given by (24).

$$\begin{aligned}u_{sm\_1eq} &= L_g C_f \left[ v_1 - 2\omega i_q \cdot C_f^{-1} + \left( (L_g C_f)^{-1} + \omega^2 \right) v_{ld} + \dot{i}_{ld} \cdot C_f^{-1} + i_{lq} \omega \cdot C_f^{-1} \right] \\ u_{sm\_2eq} &= L_g C_f \left[ v_2 + 2i_d \omega \cdot C_f^{-1} + \left( (L_g C_f)^{-1} + \omega^2 \right) v_{lq} + \dot{i}_{lq} \cdot C_f^{-1} - i_{ld} \omega \cdot C_f^{-1} \right] \\ u_{sm\_3eq} &= (L_g + 3L_n) C_f \left[ v_3 + \left[ (L_g + 3L_n) C_f \right]^{-1} v_{ln} + \dot{i}_{ln} \cdot C_f^{-1} \right]\end{aligned}\quad (24)$$

It is important to ensure that the values obtained for the equivalent control align with (19). To regulate the state variables on the sliding surface, the conditions  $s_1 = s_2 = s_3 = 0$  and  $\gamma_1 > 0, \gamma_2 > 0, \gamma_3 > 0$  must be satisfied. If  $s_1, s_2, s_3 \neq 0$ , the control strategy is defined as (25).

$$\begin{aligned} u_{sm\_1} &= u_{sm\_1eq} + \gamma_1 \text{sign}(s_1) \\ u_{sm\_2} &= u_{sm\_2eq} + \gamma_2 \text{sign}(s_2) \\ u_{sm\_3} &= u_{sm\_3eq} + \gamma_3 \text{sign}(s_3) \end{aligned} \tag{25}$$

Substituting (23) into (20) yields the following set of (26).

$$\begin{aligned} \dot{s}_1 &= -\gamma_1 \text{sign}(s_1) \\ \dot{s}_2 &= -\gamma_2 \text{sign}(s_2) \\ \dot{s}_3 &= -\gamma_3 \text{sign}(s_3) \end{aligned} \tag{26}$$

To address the complexity of the controller arising from the use of discontinuous functions,  $u_{sm-sw}$ , each sliding surface only needs to regulate the speed to reach the average switching level through a basic LCL filter [6]. The system’s stability and robustness can be evaluated using the Lyapunov function, as proposed by Slotine and Li [27], defined as (27).

$$\bar{u}_{sm\_ieq} = \frac{\omega_0}{s + \omega_0} u_{sm-sw\_i} = \begin{cases} \frac{\omega_0}{s + \omega_0} u_{sm\_imax}^+, S_i > 0 \\ \frac{\omega_0}{s + \omega_0} u_{sm\_imax}^-, S_i < 0 \end{cases} \tag{27}$$

Here,  $\omega_0 = 2\pi f_0$  rad/s represents the cut-off frequency of the passive filter. To prevent system delays and oscillations, the cut-off frequency must be carefully chosen—not excessively high or low. Accordingly,  $f_0$  is set to 2 kHz to effectively suppress oscillations, even when the values of  $u_{sm\_1max}^+, u_{sm\_1min}^+, u_{sm\_2max}^+, u_{sm\_2min}^+, u_{sm\_3max}^+$ , and  $u_{sm\_3min}^+$  reach the steady-state control inputs ( $u_{sm\_1st}, u_{sm\_2st}, u_{sm\_3st}$ ). The steady-state condition is defined in (28).

$$\begin{aligned} u_{sm\_1st} &= (2\omega i_q - \omega i_{lq}) \cdot (L_g^{-1} + C_f \omega^2)^{-1} \\ u_{sm\_2st} &= (2\omega i_d - \omega i_{ld}) \cdot [L_g^{-1} + C_f \omega^2]^{-1} \\ u_{sm\_3st} &= 0 \end{aligned} \tag{28}$$

The values of  $u_{sm\_1max}^+$  and  $u_{sm\_1min}^+$  are defined as  $u_{sm\_imax}^+ = u_{sm\_ist} + \Delta_i$  and  $u_{sm\_imin}^+ = u_{sm\_ist} - \Delta_i$ , respectively, where  $\Delta_i$  is a constant introduced to preserve system stability. Consequently, the extent of system oscillation is directly influenced by the magnitude of  $\Delta_i$ . In summary, the input functions in (25) are modified as (29), in which the coefficients  $\gamma_1, \gamma_2$ , and  $\gamma_3$  ensure the existence of mode sliding on the surface.

$$\begin{aligned} u_{sm\_1} &= \bar{u}_{sm\_1eq} + \gamma_1 \text{sign}(s_1) \\ u_{sm\_2} &= \bar{u}_{sm\_2eq} + \gamma_2 \text{sign}(s_2) \\ u_{sm\_3} &= \bar{u}_{sm\_3eq} + \gamma_3 \text{sign}(s_3) \end{aligned} \tag{29}$$

Figure 2 presents the structure of the linearized input feedback–sliding mode output control, focusing on the reference value along the d-axis ( $v_{id}^*$ ). When the voltage source inverter (VSI) delivers a balanced three-phase output, the remaining reference values are set to zero.

**4. SIMULATED PERFORMANCE**

Each controller is tested through two simulation runs incorporating an active power filter. The first scenario employs PI control, while the second utilizes sliding mode (SM) control. To evaluate the effectiveness of the proposed approach, simulations are conducted using the PSIM software, targeting both unbalanced and nonlinear load conditions. The input source is a three-phase AC grid (380 V, 50 Hz), and the inverter operates at a switching frequency of 10 kHz. The LCL filter parameters, detailed in Table 1, are designed for a cut-off frequency of 450 Hz. Table 2 outlines the load specifications and controller settings, while Table 3 presents the simulation outcomes for both PI and SM control strategies.

Table 1. Configuration details of the VSI and LCL filter

Parameters	Value	Filter type
$L_f$	1.083 [mH]	LCL
$C_f$	120 [uF]	LCL
$L_g$	3.0 [mH]	LCL
$C_{cd1}$	4700 [uF]	VSI
$C_{cd2}$	4700 [uF]	VSI

Table 2. Controller configuration settings

Gain/load parameters		Gain	
Controller type		Non-linear load: $L = 0.3$ [mH], $C = 0.47$ [mF], $R = 0.5$ [ $\Omega$ ]	Unbalanced non-linear load: $L_a = L_b = L_c = 0.3$ [mH], $C_a = C_b = C_c =$ $0.47$ [mF], $R_a = R_c = 5$ [ $\Omega$ ], $R_b = 25$ [ $\Omega$ ]
PI control	Current controller	$k_p = 12.7$ ; $k_i = 11200$	$k_p = 17.7$ ; $k_i = 13150$
	Voltage controller	$k_{pv} = 0.31$ ; $k_{iv} = 815$	$k_{pv} = 0.35$ ; $k_{iv} = 898$
	SM control	$\eta_{11} = \eta_{21} = \eta_{31} = 5 * 10^3$ and $\eta_{12} = \eta_{22} = \eta_{32} = 8.4 * 10^6$	

Table 3. THD<sub>sm</sub> comparison across different loads and controllers

Load type	Controller type	THD [%]		
		THD phase A	THD phase B	THD phase C
Non-linear load	PI	2.15	2.55	2.52
	SM	2.12	2.37	2.14
Unbalanced non-linear load	PI	1.97	5.02	1.89
	SM	1.5	4.09	1.66

The simulation outcomes depicted in Figures 3 through 8 reveal several key observations: first, the phase load voltage remains consistently balanced under control. Second, system currents adhere to Kirchhoff’s current laws, as demonstrated by (1)-(3). Third, the proposed control method achieves lower total harmonic distortion (THD) in the phase load currents compared to PI control, across both nonlinear and unbalanced nonlinear load conditions.

The simulation results emphasize the behavior of the three-phase grid and load currents. Figures 4 and 7 illustrate the voltage of phase a ( $v_{F\_aN}$ ) and line a ( $v_{F\_ab}$ ) of the VSI under different load conditions. Table 3 highlights the significant difference in THD between the two controllers when subjected to an unbalanced linear load. Specifically, the PI controller reduced the a-phase load voltage THD from 2.15% to 1.97%, while the SM controller achieved a greater reduction from 2.12% to 1.5%, as shown in Figures 5 and 8. In comparison, Table 2 shows that under unbalanced nonlinear load conditions—particularly with phase b imbalance—the THD of  $i_b$  is notably higher than in other cases. However, with the SM controller, it remains below 5%, as depicted in Figure 8. This lower THD confirms that the SM control method outperforms the PI controller in managing both nonlinear and unbalanced nonlinear loads.

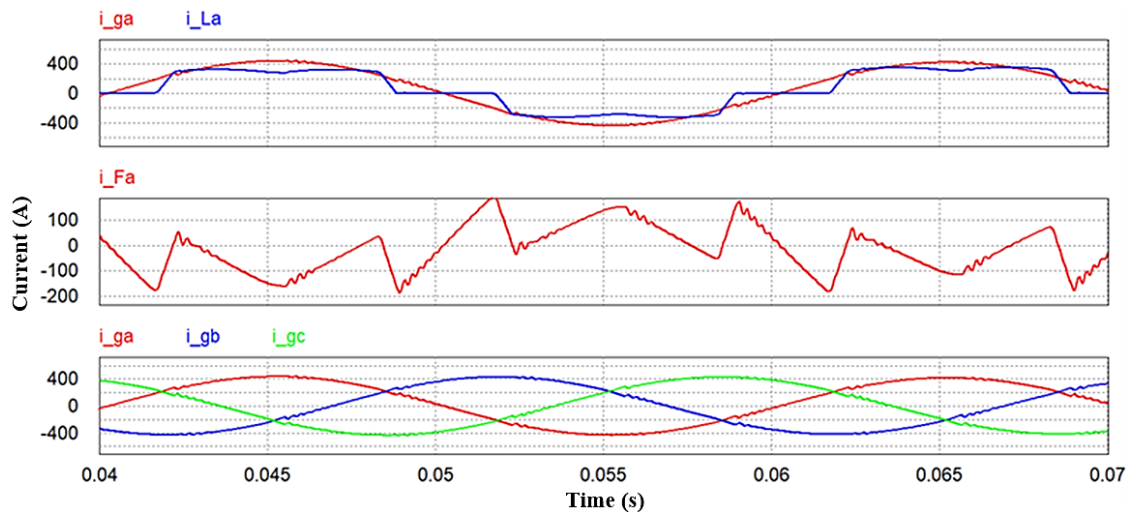


Figure 3. Transient behavior of the proposed SM controller under nonlinear loading: grid current ( $i_{gj}$ ), filter current ( $i_{Fj}$ ), and load current ( $i_{Lj}$ )



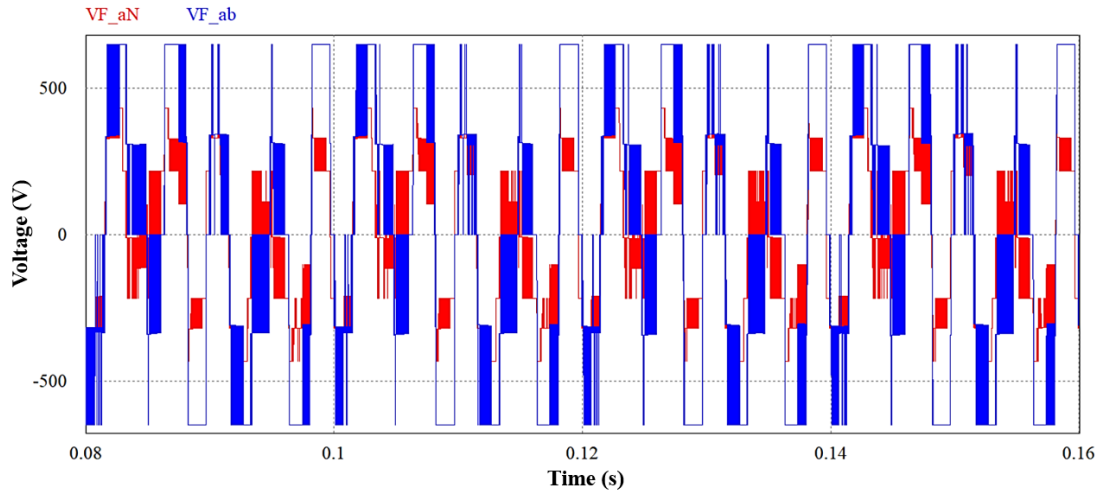


Figure 4. Transient response of VSI phase-a voltage under nonlinear load using the proposed SM controller

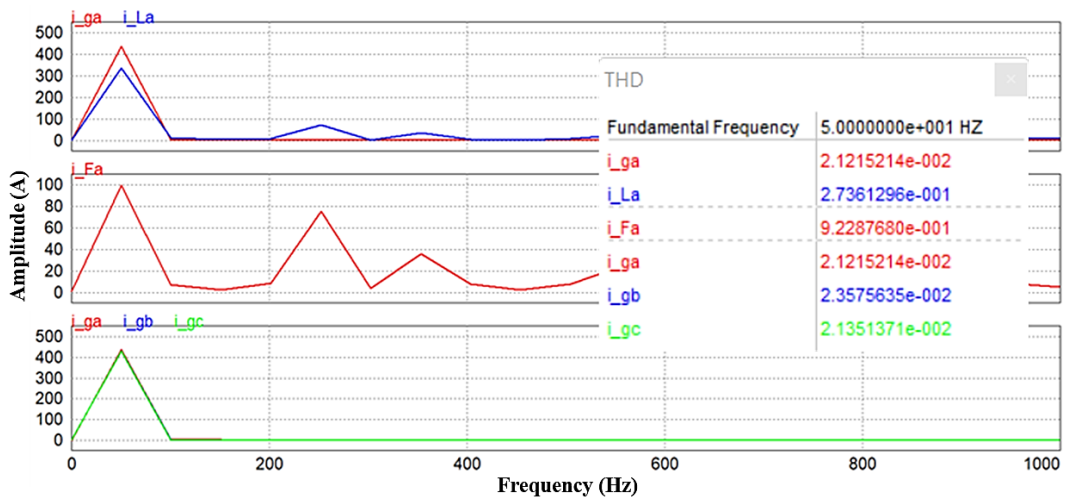


Figure 5. Dynamic behavior of current THD under nonlinear load using the proposed SM controller

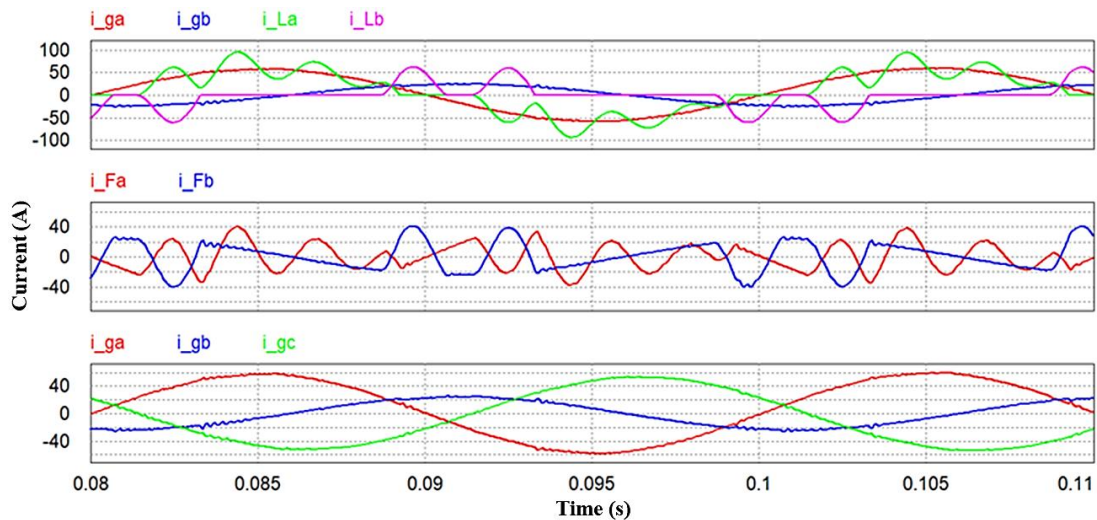


Figure 6. Response of grid, filter, and load currents ( $i_{gj}$ ,  $i_{Fj}$ ,  $i_{Lj}$ ) under unbalanced nonlinear load using the proposed SM controller

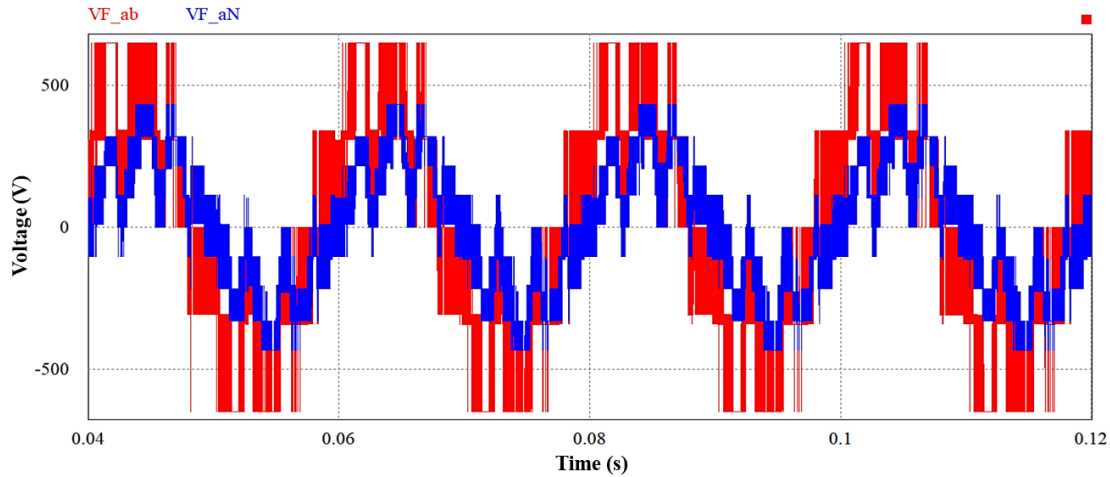


Figure 7. Voltage response at VSI phase-*a* under an unbalanced nonlinear load with the proposed sliding mode controller

Figures 7 and 8 depict the response signals of  $i_{gb}$ . Initially, high signal levels may adversely impact device performance; however, this issue can be mitigated using a delay timer switch. According to Lyapunov stability theory [27] and the 5% standard control criterion, a stable  $i_{gb}$  response exceeding 85% is achieved at approximately  $3.06 \times 10^{-2}$  seconds from startup—equivalent to around 1.5 cycles of the fundamental frequency—as illustrated in Figure 6. The deviation between the reference signal  $i_{sine_b}$  and the actual response  $i_{gb}$  is 0.77 A for the SM controller and 5.3 A for the PI controller, indicating superior tracking performance of the SM method.

In accordance with the IEEE 1992 standards for total harmonic distortion (THD), overshoot and its corresponding response time are key performance indicators in control systems—especially in active power filter (APF) applications dealing with unbalanced nonlinear loads. By applying Lyapunov’s function, these parameters were precisely calculated and are illustrated in Figures 9 and 10. The proposed sliding mode (SM) control method was evaluated across a load power range of 5 to 48 kW, as shown in Figure 11. The results demonstrate a significant reduction in THD, from 4.83% to 2.12%, maintaining values below the 5% threshold and thereby satisfying IEEE compliance. These findings confirm the superior performance and robustness of the SM control technique under challenging load conditions.

The load range for each control approach is illustrated in Figure 11, demonstrating that the SM control technique delivers better results than the PI method. Here, PI and SM/NNL represent PI and SM control methods under nonlinear load conditions, while PI and SM/unb\_NNL represent PI and SM control under unbalanced nonlinear load conditions.

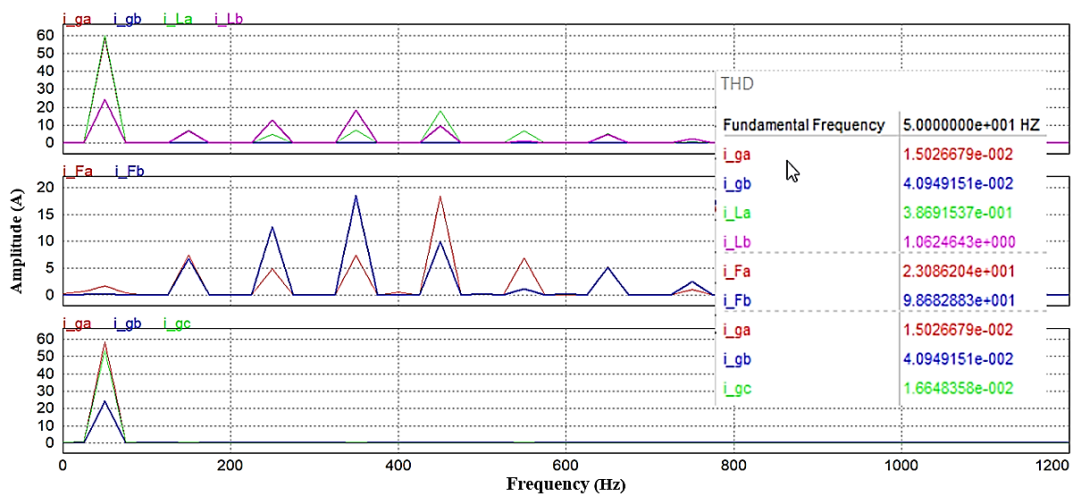


Figure 8. Dynamic response of proposed SM controller under unbalanced non-linear load: current THD

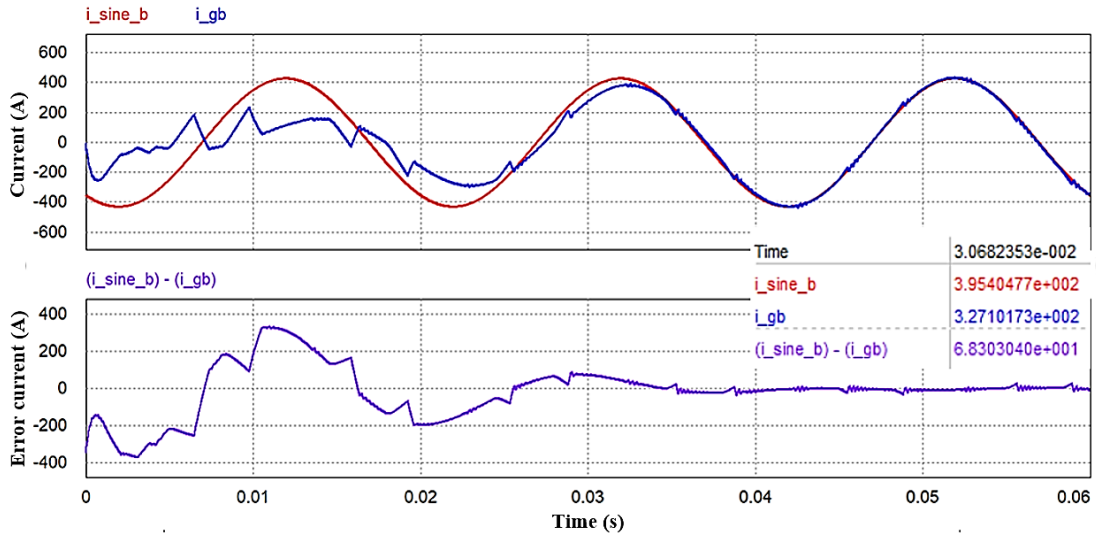


Figure 9. Peak deviation and corresponding response time of the SM controller for the nonlinear load

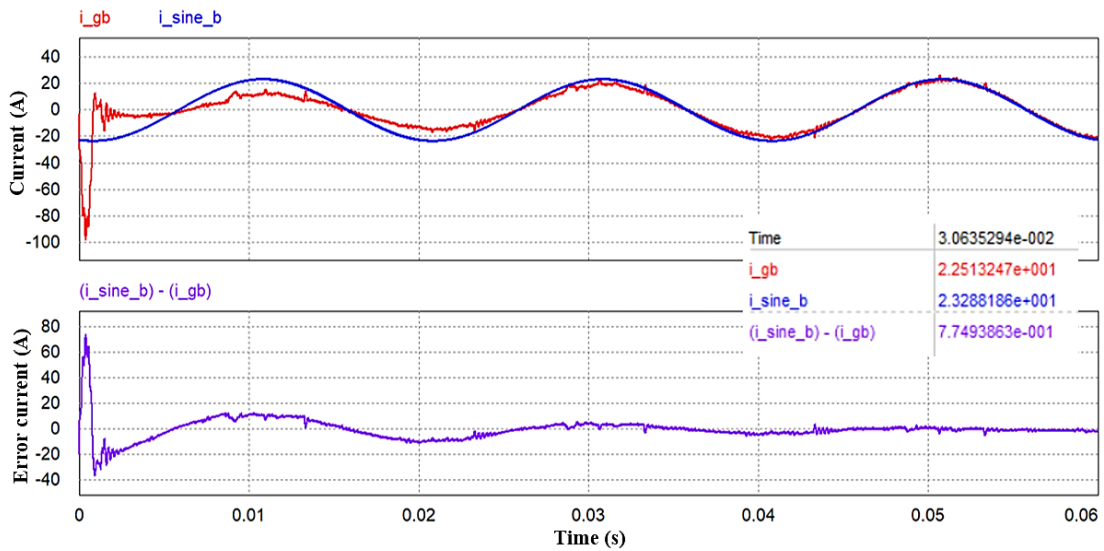


Figure 10. Overshoot and response time of the proposed SM controller under unbalanced nonlinear load conditions

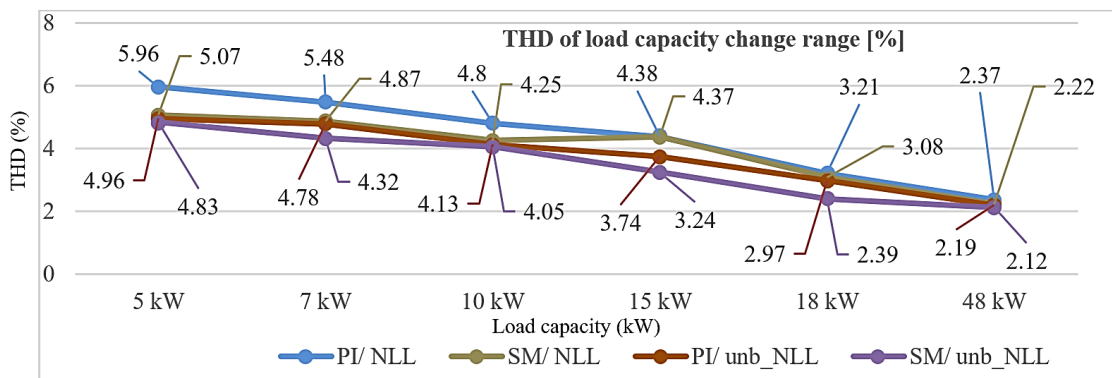


Figure 11. Evaluation of THD performance for PI and SM controllers with changing load capacities

## 5. CONCLUSION

This paper presents a self-adaptive control strategy for a three-phase, four-wire active power filter (APF) system, designed to meet the need for a simple yet efficient algorithm. The proposed model employs a sliding mode input-output feedback linearization method, enabling dynamic load adjustment under both balanced and unbalanced nonlinear conditions. To address the limitations of conventional linear controllers, feedback linearization was applied, resulting in an extended load handling range—from 5 kW to 48 kW or more—while maintaining THD below 5%, in compliance with power quality standards.

Due to the complexity of APF system calculations, the sliding mode approach was adopted to simplify the controller structure. An LCL filter was also integrated to mitigate load-induced noise, which can degrade control performance. Although the response time of the proposed control method for three-phase VSI capacitors remains relatively slow (approximately 1.5 cycles of the fundamental signal to reach steady state), simulation results confirmed its effectiveness. The SM controller demonstrated superior performance compared to traditional PI methods, achieving lower THD (maximum  $\text{THD}_{\text{sm}} = 4.96\%$ ) and better adaptability to nonlinear and unbalanced load variations. Future work will focus on enhancing the controller's self-tuning capabilities by integrating a fuzzy PI controller, aiming to improve performance in the presence of higher-order harmonics.

## FUNDING INFORMATION

This research was funded by the joint collaborative research program between Sai Gon University (SGU) and the University of Transport Ho Chi Minh City in Vietnam.

## AUTHOR CONTRIBUTIONS STATEMENT

This journal uses the Contributor Roles Taxonomy (CRediT) to recognize individual author contributions, reduce authorship disputes, and facilitate collaboration.

Name of Author	C	M	So	Va	Fo	I	R	D	O	E	Vi	Su	P	Fu
Leminh Thien Huynh	✓	✓	✓	✓	✓	✓	✓	✓	✓	✓	✓	✓	✓	✓
Van-Cuu Ho		✓				✓		✓	✓		✓	✓		
Thanh-Vu Tran	✓		✓	✓			✓			✓	✓		✓	✓

C : **C**onceptualization

M : **M**ethodology

So : **S**oftware

Va : **V**alidation

Fo : **F**ormal analysis

I : **I**nvestigation

R : **R**esources

D : **D**ata Curation

O : Writing - **O**riginal Draft

E : Writing - Review & **E**ditng

Vi : **V**isualization

Su : **S**upervision

P : **P**roject administration

Fu : **F**unding acquisition

## CONFLICT OF INTEREST STATEMENT

The authors declare that they have no known competing financial interests or personal relationships that could have appeared to influence the work reported in this paper. The research was conducted independently and objectively, without any financial, professional, or personal conflict of interest.

## DATA AVAILABILITY




The data that support the findings of this study are available from the corresponding author, [LTH], upon reasonable request. All simulation models, figures, and analysis scripts were developed by the authors as part of this study and can be shared for academic and non-commercial purposes.

## REFERENCES




- [1] IEEE Standards Association, *IEEE recommended practice and requirements for harmonic control in electric power systems*, IEEE Std 519-2014, Piscataway, NJ, USA: IEEE, Mar. 27, 2014, doi: 10.1109/IEEESTD.2014.6826459.
- [2] S. Salas-Duarte, I. Araujo-Vargas, J. Ramirez-Hernandez, and M. Rivera, "Evaluation of a trapezoidal predictive controller for a four-wire active power filter for utility equipment of metro railway, power-land substations," *Mathematical Problems in Engineering*, vol. 2016, pp. 1–11, 2016, doi: 10.1155/2016/2712976.

- [3] A. Bag, B. Subudhi, and P. K. Ray, "Comparative analysis of sliding mode controller and hysteresis controller for active power filtering in a grid connected PV system," *International Journal of Emerging Electric Power Systems*, vol. 19, no. 1, pp. 1–13, Feb. 2018, doi: 10.1515/ijeeps-2017-0044.
- [4] S. R. Das *et al.*, "A comprehensive survey on different control strategies and applications of active power filters for power quality improvement," *Energies*, vol. 14, no. 15, p. 4589, Jul. 2021, doi: 10.3390/en14154589.
- [5] F. Garcia-Torres, S. Vazquez, I. M. Moreno-Garcia, A. Gil-de-Castro, P. Roncero-Sanchez, and A. Moreno-Munoz, "Microgrids power quality enhancement using model predictive control," *Electronics*, vol. 10, no. 3, p. 328, Feb. 2021, doi: 10.3390/electronics10030328.
- [6] L. T. Huynh, T. V. Tran, V. D. Do, and V. C. Ho, "Active power filter under imbalance and distortion of grid connected solution," in *International Conference on Industrial Networks and Intelligent Systems*, 2021, pp. 348–366, doi: 10.1007/978-3-030-77424-0\_29.
- [7] S. Peresada, Y. Zaichenko, and S. Dymko, "Selective estimation of three-phase mains current for shunt active power filter," in *2020 IEEE 7th International Conference on Energy Smart Systems (ESS)*, IEEE, May 2020, pp. 68–72, doi: 10.1109/ESS50319.2020.9160201.
- [8] E. Sundaram, M. Gunasekaran, R. Krishnan, S. Padmanaban, S. Chenniappan, and A. H. Ertas, "Genetic algorithm based reference current control extraction based shunt active power filter," *International Transactions on Electrical Energy Systems*, vol. 31, no. 1, p. e12623, Jan. 2021, doi: 10.1002/2050-7038.12623.
- [9] H. L. M. Thien, D. Van Huong, N. X. Tien, H. Van Cuu, and T. T. Vu, "Improving the electric quality of the back-to-back system on modern electric railways using active power filter algorithm," *Journal of Mechanical Engineering Research and Developments*, vol. 44, no. 1, pp. 83–98, 2020.
- [10] A. Naderipour, A. A. M. Zin, M. H. B. Habibuddin, M. R. Miveh, and J. M. Guerrero, "An improved synchronous reference frame current control strategy for a photovoltaic grid-connected inverter under unbalanced and nonlinear load conditions," *PLOS ONE*, vol. 12, no. 2, p. e0164856, Feb. 2017, doi: 10.1371/journal.pone.0164856.
- [11] I. Ullah and M. Ashraf, "Sliding mode control for performance improvement of shunt active power filter," *SN Applied Sciences*, vol. 1, no. 6, p. 531, Jun. 2019, doi: 10.1007/s42452-019-0554-9.
- [12] J. L. Flores-Garrido, P. Salmerón, and J. A. Gómez-Galán, "Nonlinear loads compensation using a shunt active power filter controlled by feedforward neural networks," *Applied Sciences*, vol. 11, no. 16, p. 7737, Aug. 2021, doi: 10.3390/app11167737.
- [13] Y. Yang and R.-J. Wai, "Design of adaptive fuzzy-neural-network-imitating sliding-mode control for parallel-inverter system in islanded micro-grid," *IEEE Access*, vol. 9, pp. 56376–56396, 2021, doi: 10.1109/ACCESS.2021.3071832.
- [14] J. Chen, H. Shao, and C. Liu, "An improved deadbeat control strategy based on repetitive prediction against grid frequency fluctuation for active power filter," *IEEE Access*, vol. 9, pp. 24646–24657, 2021, doi: 10.1109/ACCESS.2021.3057386.
- [15] H. Geng, T. Zou, and A. Chandra, "Fast repetitive control scheme for shunt active power filter in synchronous rotational frame," in *2017 IEEE Industry Applications Society Annual Meeting*, IEEE, Oct. 2017, pp. 1–6, doi: 10.1109/IAS.2017.8101732.
- [16] J. Fei and D. Cao, "Adaptive fractional terminal sliding mode controller for active power filter using fuzzy-neural-network," in *2018 10th International Conference on Knowledge and Systems Engineering (KSE)*, IEEE, Nov. 2018, pp. 118–122, doi: 10.1109/KSE.2018.8573380.
- [17] E. Nwokolo, I. Chinaeke-Ogbuka, A. Ajibo, C. Ogbuka, U. Ogbuefi, and E. Ejiogu, "Performance comparison of sliding mode and instantaneous reactive power theory control techniques for three-phase active power filter," *International Journal of Electrical and Electronic Engineering and Telecommunications*, vol. 10, no. 2, pp. 83–90, 2021, doi: 10.18178/ijeetc.10.2.83-90.
- [18] A. Qashou, S. Yousef, A. A. Smadi, and A. A. AlOmari, "Distribution system power quality compensation using a HSeAPF based on SRF and SMC features," *International Journal of System Assurance Engineering and Management*, vol. 12, no. 5, pp. 976–989, Oct. 2021, doi: 10.1007/s13198-021-01185-w.
- [19] A. Sahara, A. Kessal, L. Rahmani, and J.-P. Gaubert, "Improved sliding mode controller for shunt active power filter," *Journal of Electrical Engineering and Technology*, vol. 11, no. 3, pp. 662–669, May 2016, doi: 10.5370/JEET.2016.11.3.662.
- [20] Y. Belkhier, A. Achour, R. N. Shaw, N. Ullah, M. S. Chowdhury, and K. Techato, "Energy-based combined nonlinear observer and voltage controller for a PMSG using fuzzy supervisor high order sliding mode in a marine current power system," *Sustainability*, vol. 13, no. 7, p. 3737, Mar. 2021, doi: 10.3390/su13073737.
- [21] M. A. E. Mohamed, S. A. Ward, M. F. El-Gohary, and M. A. Mohamed, "Hybrid fuzzy logic-PI control with metaheuristic optimization for enhanced performance of high-penetration grid-connected PV systems," *Scientific Reports*, vol. 15, no. 1, p. 24650, Jul. 2025, doi: 10.1038/s41598-025-09336-w.
- [22] O. Khentaoui *et al.*, "Adaptive backstepping controller based on energy concept of shunt active power filter connected to PV system," *Electrical Engineering*, vol. 107, no. 6, pp. 7737–7758, Jun. 2025, doi: 10.1007/s00202-024-02931-6.
- [23] H. L. M. Thien, N. X. Tien, T. T. Vu, and H. V. Cuu, "Improved the adaptation for three phase active filter under non-ideal-load using sample current control," *Journal of Mechanical Engineering Research and Developments*, vol. 42, no. 3, pp. 76–80, Apr. 2019, doi: 10.26480/jmerd.03.2019.76.80.
- [24] K. Srinitha, M. F. Saleem, G. Priyanka, and A. Srinivas, "Power quality improvement using dynamic voltage restorer with sliding mode control," *International Journal of Engineering and Science Research*, vol. 14, no. 2, pp. 144–153, 2024.
- [25] P. Santiprapan, K. Areerak, and K. Areerak, "Dynamic model of active power filter in three-phase four-wire system," in *2014 11th International Conference on Electrical Engineering/Electronics, Computer, Telecommunications and Information Technology (ECTI-CON)*, IEEE, May 2014, pp. 1–5, doi: 10.1109/ECTICon.2014.6839776.
- [26] T.-V. Tran, T.-W. Chun, H.-H. Lee, H.-G. Kim, and E.-C. Nho, "PLL-based seamless transfer control between grid-connected and islanding modes in grid-connected inverters," *IEEE Transactions on Power Electronics*, vol. 29, no. 10, pp. 5218–5228, Oct. 2014, doi: 10.1109/TPEL.2013.2290059.
- [27] J.-J. Slotine and W. Li, *Applied nonlinear control*. Englewood Cliffs, NJ, USA: Prentice-Hall, 1991.
- [28] Y. Chen, S. Li, and J. Fei, "Adaptive backstepping second-order sliding mode fuzzy control for three-phase active power filter," *Advances in Mechanical Engineering*, vol. 11, no. 11, pp. 1–8, Nov. 2019, doi: 10.1177/1687814019890797.
- [29] J. Zhuo, C. An, and J. Fei, "Fuzzy multiple hidden layer neural sliding mode control of active power filter with multiple feedback loop," *IEEE Access*, vol. 9, pp. 114294–114307, 2021, doi: 10.1109/ACCESS.2021.3104030.
- [30] I. Boussadia, K. Saoudi, Z. Bouchama, I. Aliskan, I. Griche, and M. Ayad, "A backstepping sliding mode control of DC-DC buck converter," *Przegląd Elektrotechniczny*, vol. 1, no. 6, pp. 88–91, Jun. 2024, doi: 10.15199/48.2024.06.16.




**BIOGRAPHIES OF AUTHORS**

**Leminh Thien Huynh**    received an associate's degree in telecommunications electronics from PTIT Ho Chi Minh City in 2003. He received a B.Eng. degree in electrical and electronic engineering and an M.S. degree in electronic engineering from UTE, Vietnam, in 2004 and 2011, respectively. He received his Ph.D. degree in automation and control engineering from the University of Transport Ho Chi Minh City, Vietnam, in 2023. He is currently a lecturer at the Faculty of Engineering and Technology at Saigon University, Ho Chi Minh City, Vietnam. His research interests include power quality control, adaptive control, fuzzy logic control, machine learning, renewable energy, and electric vehicles (EVs). He can be contacted at email: [leminhthien.huynh@sgu.edu.vn](mailto:leminhthien.huynh@sgu.edu.vn).



**Van-Cuu Ho**    received his B.S. and M.S. degrees in electronics communication engineering from the Ho Chi Minh University of Technology, Ho Chi Minh City, Vietnam, in 1987 and 1997, respectively. He received a Ph.D. degree in network industry and information channels from the Hanoi Polytechnic University, Hanoi Polytechnic University, Vietnam, in 2006. He is currently Dean of the Faculty of Engineering and Technology at Saigon University, Hochiminh City, Vietnam. He can be contacted at email: [cuuhovan@sgu.edu.vn](mailto:cuuhoven@sgu.edu.vn) or [cuuhovan@gmail.com](mailto:cuuhoven@gmail.com).



**Thanh-Vu Tran**    received his B.S. and M.S. degrees in electronics and electrical engineering from the Ho Chi Minh University of Technology, Ho Chi Minh City, Vietnam, in 2005 and 2008, respectively. He received his Ph.D. degree in electrical engineering from the University of Ulsan, Ulsan, Korea, in 2013. He finished his postdoctoral program at the University of Ulsan in 2015. His current research interests include power converter topologies, the control of power converters, renewable energy, control of grid-connected inverter systems, and energy efficiency. He can be contacted at email: [vu.tran@ut.edu.vn](mailto:vu.tran@ut.edu.vn).